Molecular Biology of the Cell
Vol. 15, 973–981, March 2004

Fibronectin Matrix Assembly Regulates α5β1-mediated Cell Cohesion

Elizabeth E. Robinson, Ramsey A. Foty, and Siobhan A. Corbett*

Department of Surgery, UMDNJ-Robert Wood Johnson Medical School, New Brunswick, New Jersey 08903

Submitted July 25, 2003; Revised November 25, 2003; Accepted December 2, 2003
Monitoring Editor: Jean Schwarzbauer

Integrin-extracellular matrix (ECM) interactions in two-dimensional (2D) culture systems are widely studied (Goldstein and DiMilla, 2002. J Biomed. Mater. Res. *59,* 665–675; Koo *et al.,* 2002. J. Cell Sci. *115,* 1423–1433). Less understood is the role of the ECM in promoting intercellular cohesion in three-dimensional (3D) environments. We have demonstrated that the α5β1-integrin mediates strong intercellular cohesion of 3D cellular aggregates (Robinson *et al.,* 2003. J. Cell Sci. *116,* 377–386). To further investigate the mechanism of α5β1-mediated cohesivity, we used a series of chimeric α5β1-integrin–expressing cells cultured as multilayer cellular aggregates. In these cell lines, the α5 subunit cytoplasmic domain distal to the GFFKR sequence was truncated, replaced with that of the integrin α4, the integrin α2, or maintained intact. Using these cells, α5β1-integrin–mediated cell aggregation, compaction and cohesion were determined and correlated with FN matrix assembly. The data presented demonstrate that cells cultured in the absence of external mechanical support can assemble a FN matrix that promotes integrin-mediated aggregate compaction and cohesion. Further, inhibition of FN matrix assembly blocks the intercellular associations required for compaction, resulting in cell dispersal. These results demonstrate that FN matrix assembly contributes significantly to tissue cohesion and represents an alternative mechanism for regulating tissue architecture.

INTRODUCTION

Integrin-fibronectin (FN) interactions are essential to a diverse number of important cellular behaviors underlying embryogenesis (Lash *et al.,* 1984; Downie and Newman, 1995), wound healing (Grinnell *et al.,* 1981; Clark, 1990), cell migration (Hynes, 1990), and metastasis (Akamatsu *et al.,* 1996; Armstrong and Armstrong, 2000). FN is a multifunctional, adhesive glycoprotein that is secreted by cells as a soluble dimer and that can be assembled on the cell surface into mesh-like fibrils (Hynes, 1990). FN fibrillogenesis is initiated by the binding of the integrin α5β1 to the Arg-Gly-Asp (RGD) and synergy sites located within the cell-binding domain of each FN subunit (Akiyama *et al.,* 1995). In the absence of α5β1 expression, αv integrins can replace the role of α5β1 in FN matrix assembly (Yang *et al.,* 1993; Yang and Hynes, 1996). Integrin-FN interaction results in a conformational change in the FN molecule exposing self-association sites. Receptor clustering and increased concentration of localized FN allows for fibril formation, propagation, and ultimately, the generation of a detergent-insoluble FN matrix composed of high-molecular-weight FN multimers (Schwarzbauer, 1991; Morla and Ruoslahti, 1992; Hocking *et al.,* 1994; Wierzbicka-Patynowski and Schwarzbauer, 2003). The analysis of FN matrix assembly has relied largely on assays in which adherent cells are cultured on two-dimensional (2D) substrates (Sechler *et al.,* 1996; Sechler and Schwarzbauer, 1997). Such assays have significantly contributed to our understanding of the structural requirements of the matrix assembly process. Few studies however, have addressed the role of FN matrix assembly in a three-dimensional (3D) environment that more closely reflects in vivo tissue architecture. In this context, FN fibrils that link adjacent cells could potentially contribute to tissue compaction and cohesivity.

Tissue compaction and cohesivity are essential to a variety of important biological processes. In the developing embryo, for example, they play vital roles in early and late morphogenetic processes, including blastomere formation (Richa *et al.,* 1985; Fleming *et al.,* 2001), somitogenesis (Lash *et al.,* 1984), forelimb development (Downie and Newman, 1995; Adamska *et al.,* 2003), and heart development (Khan *et al.,* 2003). In adult organisms, the compaction of granulation tissue contributes to wound closure and wound remodeling (Berry *et al.,* 1998). Interestingly, increased FN expression and deposition both during embryogenesis and during wound repair is observed at sites of tissue compaction and appears to correlate spatiotemporally with this process. For example, a correlation exists between high FN secretion and the aggregation of the precartilage mesenchymal cells during wing and leg bud development (Downie and Newman, 1995). Similarly during the early stages of somitogenesis in the chick embryo, the presomitic cells in the segmental plate undergo FN-dependent compaction (Lash *et al.,* 1984). During wound healing, abundant FN is deposited in granulation tissue, which has been shown to condense and contribute to the closure of open wounds (Grinnell *et al.,* 1981; Clark, 1990). Further, in vitro models of wound healing have shown that FN is required for the efficient contraction of cell-populated 3D collagen or fibrin lattices (Corbett and Schwarzbauer, 1999; Hocking *et al.,* 2000).

Our recent work has demonstrated that the α5β1-integrin mediates strong intercellular cohesion of 3D cellular aggregates (Robinson *et al.,* 2003). To further investigate the mechanism of α5β1-mediated cohesivity, we used a series of

Article published online ahead of print. Mol. Biol. Cell 10.1091/mbc.E03–07–0528. Article and publication date are available at www.molbiolcell.org/cgi/doi/10.1091/mbc.E03–07–0528.

* Corresponding author. E-mail address: corbetsi@umdnj.edu.

chimeric α5β1-integrin–expressing cells, cultured in 3D. In these cell lines, the α5 subunit cytoplasmic domain distal to the GFFKR sequence was truncated, replaced with that of the integrin α4, the integrin α2, or maintained intact. Using these cells, α5β1-integrin–mediated cell aggregation, compaction, and cohesion were assessed and correlated with FN matrix assembly. The data presented demonstrate that cells cultured in the absence of external mechanical support can assemble a FN matrix that promotes integrin-mediated aggregate compaction and cohesion. Inhibition of FN matrix assembly blocks the intercellular associations required for compaction, resulting in cell dispersal. These results provide a relevant in vitro model with which to analyze the role of FN matrix assembly in tissue cohesion.

MATERIALS AND METHODS

Construction of Chimeric Integrin Plasmids

Three chimeric plasmids were generated encoding the extracellular and transmembrane domains of α5-integrin (X5) and either a truncated cytoplasmic domain (X5C0), the cytoplasmic domain of α2-integrin (X5C2), or the cytoplasmic domain of α4-integrin (X5C4). The chimeric constructs were generated as follows. The wild-type human α4-integrin subunit, X4C4, the chimeric X4C2 cDNA, in which the coding region for the α4 cytoplasmic domain was replaced with that of the α2-integrin, and the X4C0 cDNA, encoding the wild-type human α4-integrin subunit with a stop codon inserted just past the GFFKR sequence, were kindly provided by Dr. Patricia Keeley (University of Wisconsin, Madison, WI). A *Kpn*I-*Xba*I fragment of X4C4, X4C2, or X4C0, containing the cytoplasmic portion of the receptor was cloned into pcDNA 3.1 to generate pcDNA 3.1 C4, C2, or C0 respectively. A 3.1-kb *Hin*dIII digest of X5C5 was then used to generate X5. This *Hin*dIII fragment was cloned into *Hin*dIII-digested pcDNA 3.1 C4, C2, or C0, to yield X5C4, X5C2, or X5C0, respectively. The cytoplasmic portions of X5C4, X5C2, and X5C0 were sequenced at the Robert Wood Johnson Medical School DNA Core Facility to confirm the sequences.

Generation of Chimeric Integrin-expressing CHO-B2 Cells

Cells were transfected by electroporation using a Bio-Rad Gene Pulser II apparatus (Bio-Rad Laboratories, Hercules, CA) at 200 V and 960 μF in transfection medium (RPMI, 0.1 mM DTT, 10 mM dextrose) with 20 μg of chimeric constructs. Transfected cells were grown to confluence in medium supplemented with 800 μg/ml G418 and bulk sorted using a fluorescence-activated cell sorter (FACS; EPICS ALTRA, Beckman Coulter, Miami, FL) to generate populations that expressed similar levels of the chimeric integrins. Empty vector control cells (P3; pcDNA3 only) were also generated by electroporation and antibiotic selection.

Flow Cytometry and FACS

Cells were detached from a near-confluent tissue culture plate with trypsin-EDTA (TE; Invitroben, Carlsbad, CA), washed three times with ice-cold HBSS and incubated with 5 μg/ml anti-human integrin α5 antibody (clone VC5; BD-PharMingen, San Diego, CA) on ice for 30 min with agitation. Cells were again washed with cold HBSS and incubated on ice for an additional 30 min with an Alexa-Fluor 488–conjugated goat anti-mouse IgG secondary antibody (Molecular Probes, Eugene, OR). Cells expressing chimeric integrins were sorted three times and expanded. Receptor expression was confirmed monthly by flow cytometry.

Confirmation of Receptor Expression by Western Blot Analysis

Cell monolayers were washed twice with ice-cold HBSS and then lysed by the addition of 500 μl RIPA lysis buffer (150 mM NaCl, 50 mM Tris, pH 7.5, 1% NP40, 0.25% deoxycholate [DOC]) containing a protease inhibitor cocktail (Calbiochem, La Jolla, CA), EDTA, and sodium vanadate. The lysates were transferred to microcentrifuge tubes, rotated at 4°C for 1 h, then passed through a Qia-shredder (Qiagen, Valencia, CA), and centrifuged at 14 × *g* for 15 min at 4°C. Lysates from 3D aggregates were prepared in the same manner except that aggregates were disrupted by sonication in RIPA lysis buffer. Protein concentrations were determined using the BCA Protein Assay Kit (Pierce, Rockford, IL). Twenty micrograms of protein was separated on a 7% SDS-PAGE gel and transferred to nitrocellulose using standard methods. Alternately, equal amounts of total cell lysate were adjusted to a concentration of 1 μg/ml with RIPA buffer and incubated with 2 μg of anti-α5 antibody (AB1950, Chemicon, Temecula, CA) at 4°C overnight. Immunocomplexes were recovered by incubating with Protein A/G-Sepharose (Pierce) for 2 h. Beads were recovered by centrifugation. The immunoprecipitates were analyzed by SDS-PAGE and transferred to nitrocellulose (Fisher Scientific, Pittsburgh, PA).

Blots were blocked overnight at 4°C in either 5% Nonfat dry milk (NFDM; X5C5, X5C4) or in membrane-blocking solution (Zymed, South San Francisco, CA; X5C2). Blots were then incubated at room temperature for 1 h in primary antibody specific for either the extracellular domain of α5 (1 μg/ml, AB 1950, Chemicon) or the cytoplasmic domain of the respective receptor (X5C5, X5C0, 1 μg/ml, AB1928, Chemicon; X5C4, 4 μg/ml, sc-6589, Santa Cruz Biotechnology, Santa Cruz, CA; X5C2, 0.5 μg/ml, AB1936, Chemicon), followed by an additional 1-h incubation with an appropriate HRP-conjugated secondary antibody. Blots were developed using SuperSignal West Pico Chemiluminescent Substrate (Pierce) and exposed to X-ray film. All blots were then stripped in 62.5 mM Tris HCl, pH 6.8, 2% SDS, and 100 mM 2-mercaptoethanol, for 30 min at 50°C and reprobed with an antiactin antibody (1:500, clone AC-40, Sigma, St. Louis, MO) to confirm equal lane loading.

Hanging Drop Assay

Cells were removed from near-confluent plates with TE, washed, and resuspended at a concentration of 2.5×10^6 cells/ml in complete medium supplemented with 2 mM $CaCl_2$. The plating density of 2.5×10^6 cells/ml is within the range described for tissue engineering purposes (Mauck *et al.*, 2002; Awad *et al.*, 2003; Dvir-Ginzberg *et al.*, 2003; 2–20 × 10^6 cells/ml). Fifteen- and 20-μl aliquots of this suspension were deposited on the underside of a 10-cm tissue culture dish lid. The lid was then inverted over 10 ml of PBS creating hanging drops. Drops were incubated under tissue culture conditions for 2–3 d, allowing the cells to coalesce at the base of the droplets and form aggregate sheets.

3D Spheroid Formation

Aggregate sheets from hanging drop assays were transferred to 10-ml shaker flasks (Bellco Glass, Vineland, NJ) and incubated under tissue culture conditions in 3 ml of complete medium on an orbital shaker at 110 rpm as previously described (Robinson *et al.*, 2003).

Quantification of Aggregate Compaction

High contrast images of aggregates were captured in IpLab imaging software (Slanalytics Inc., Fairfax, VA). A perimeter was established around each aggregate contained in the image. The number of pixels within each perimeter was recorded yielding a pixel number per aggregate, a quantifiable assessment of aggregate "size." Comparing two aggregates of the same cell number and cell size, a less compact aggregate is larger than a more compact aggregate. Therefore, the pixel number inversely correlates with aggregate compaction. Mean pixel number ± SE was measured. Statistical significance was calculated using a Student's *t* test, ANOVA, or Newman-Keul's test, as indicated. A qualitative assessment of aggregate compaction was also made.

Quantification of Aggregate Cohesivity by TST

Aggregate cohesivity was measured by tissue surface tensiometry (TST) as previously described (Foty *et al.*, 1994; Robinson *et al.*, 2003). Briefly, individual aggregates ranging in size from 540 to 800 μm in diameter were compressed between parallel plates of the tissue surface tensiometer. To minimize adhesion of aggregates to the compression plates, both the lower and upper plates were precoated with poly 2-hydroxyethylmethacrylate (poly-HEMA), a polymeric material to which cells do not adhere (Folkman and Moscona, 1978). Two main parameters were measured to determine aggregate cohesivity. First, the force with which the aggregate resisted compression at equilibrium was monitored by a Cahn recording electrobalance. Second, aggregate geometry was monitored through a 25× Nikon dissecting microscope (Garden City, NY) equipped with a CCD video camera and connected to a computer. Images of aggregates were captured, digitized, and their geometries analyzed using NIH Image software (Bethesda, MD). Each aggregate was subjected to two different degrees of compression, the second greater than the first. Measurement of aggregate geometry and the force of resistance to the compressive force were then applied to the Young-Laplace equation (Eq. 2; Foty *et al.*, 1994) in Davies, 1963), producing numerical values of *apparent* tissue surface tension (σ). A *true* surface tension is one in which the measured σ is invariant of the aggregate volume and applied force, as would be expected of a true liquid surface tension. Only those measurements of surface tension exhibiting this behavior were used to calculate aggregate cohesivity. Linear regression analysis of the data was used to determine the *r* of σ vs. volume for each cell line. Force invariance was evaluated by comparing the mean surface tension measurements after the first and second compressions (σ_1 and σ_2, respectively) of each cell line using a Student's unpaired *t* test.

Assessment of FN Matrix Assembly

The assembly of high-molecular-weight FN multimers was assessed using a DOC differential solublization protocol and Western blot analysis as previously described (Sechler *et al.*, 1996). Cells were cultured in hanging drops overnight in FN-depleted media, in the presence of 100 μg/ml FN. This concentration was chosen to ensure cell-FN-cell interactions within the short

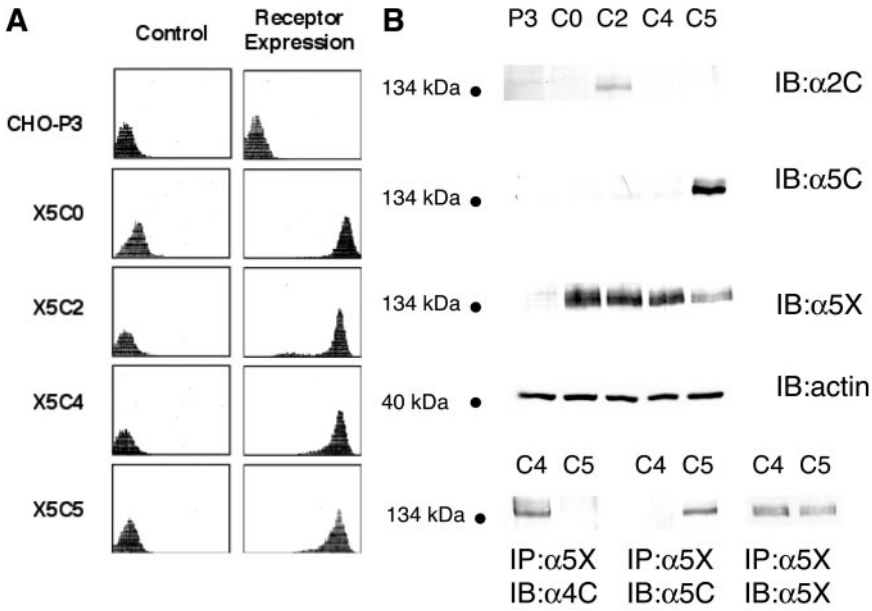

Figure 1. Determination of chimeric α5-integrin expression in transfected CHO B2 cells. (A) The X5C5, X5C4, X5C2, X5C0, and P3 cell lines were trypsinized from near confluent plates, washed and incubated with a mAb (mab) specific for the α5 extracellular domain, followed by incubation with a FITC-conjugated secondary antibody as described. The control panel (left) represents cells incubated with secondary antibody only. (B) Attached cells were lysed and total cellular lysates were analyzed by immunoblotting using a mab specific for the cytoplasmic (C) domain of the α5 or the α2 integrin. Alternately, lysates were incubated with a mab specific for the extracellular (X) domain of the α5 subunit. Immunocomplexes were recovered and analyzed by immunoblotting with a mab specific for the cytoplasmic domain of α4 or of α5, as indicated. In both cases, total lysates were analyzed by immunoblotting with a mab specific for the extracellular domain of the α5- Integrin to ensure equal loading.

time frame and to achieve a detectable signal given the small sample sizes. Cell aggregates were lysed in a DOC lysis buffer (2% sodium deoxycholate, 0.02 M Tris-HCl, pH 8.8, 2 mM PMSF, 2 mM EDTA, 2 mM iodoacetic acid, and 2 mM *N*-ethylmaleimide), passed through a 26-gauge needle, and centrifuged at 15 × *g* for 20 min at 4°C. The supernatant containing the DOC-soluble components was separated and then pelleted by centrifugation. DOC-insoluble components were solubilized using SDS lysis buffer (1% SDS, 25 mM Tris-HCl, pH 8.0, 2 mM PMSF, 2 mM EDTA, 2 mM iodoacetic acid, and 2 mM *N*-ethylmaleimide). Reduced lysates were separated on SDS-PAGE gels and probed with an anti-FN antibody (ab6584, AbCam, Ltd., Cambridge, UK). Under reducing conditions, high-molecular-weight FN multimers resolve as a 220-kDa band.

Assessment of FN Fibril Formation by Fluorescence Microscopy

Cells were trypsinized from near-confluent plates and resuspended at 2.5 × 10^6 cells/ml in FN-depleted medium. Cells were incubated FN-depleted medium, in the presence of 30 μg/ml rhodamine-labeled FN (Cytoskeleton, Inc., Denver, CO) in 15-μl hanging drops for 24 h under tissue culture conditions. Hanging drops were then transferred to glass coverslips and visualized using inverted fluorescent optics. Photographic images were captured using a Spot color camera (Diagnostic Instruments, Sterling Heights, MI) connected to a MacIntosh G4 computer (Apple Computer, Cupertino, CA) equipped with IPLab image analysis software (Scanalytics Inc.).

Inhibition of Aggregate formation by 70-kDa FN Fragment

Cells were incubated in hanging drop culture with or without 50 μg/ml exogenous rat plasma FN in the presence or absence of 50 μg/ml the 70-kDa FN fragment. Cells were imaged at 24 h and quantified by pixel number. In addition, a Western blot was performed to assess the presence of soluble and insoluble forms of FN.

RESULTS

Generation of Chimeric Integrin-expressing Cell Lines

We have previously shown that α5β1-integrin, through an RGD specific interaction with FN, can mediate the formation of spheroids and impart strong cohesivity to 3D cellular aggregates (Robinson *et al.*, 2003). To further define the mechanism of α5-integrin–mediated cohesivity, we generated CHO-B2 cells expressing chimeric α5-integrin subunits. CHO-B2 cells are null for endogenous α5-integrin expression (Schreiner *et al.*, 1989). The chimeric integrin constructs encode the extracellular, transmembrane, and juxtamembrane region of the human α5-integrin up to and including the highly conserved GFFKR sequence. Following the GFFKR sequence, either a stop codon was inserted (X5C0) or the coding region for the α5 cytoplasmic tail was replaced with that of the α2-integrin (X5C2), or that of the α4-integrin (X5C4). These constructs, in addition to the wild-type α5-integrin (X5C5), were used for transfection. Empty vector transfected cells served as a control (P3). Bulk sorting and antibiotic selection were used to establish stable populations expressing similar α5β1 receptor levels. Receptor expression stability was confirmed monthly by flow cytometry. The α5-integrin subunit is not expressed on the cell surface unless present in a heterodimer. Therefore, flow cytometry using a mAb specific for the α5-integrin subunit was used to quantify α5β1-integrin receptor expression. As demonstrated in Figure 1A, the X5C5, X5C4, X5C2, and X5C0 cell lines express similar receptor levels on the cell surface. To confirm chimeric integrin expression, lysates of attached cells (P3, X5C5, X5C0, and X5C2 cells) were analyzed by Western blot analysis using monoclonal antibodies specific for the extracellular domain of α5, the cytoplasmic domain of α5, or the cytoplasmic domain of α2 as indicated (Figure 1B, top panel). For X5C4 cells, the X5C5 or X5C4 cell lysates were immunopreciptitated with an antibody against the α5-integrin extracellular domain, and the immunocomplexes were analyzed by immunoblotting with an antibody specific for the cytoplasmic domain of α5 or of α4 (Figure 1B, bottom panel). The presence of the appropriate cytoplasmic domain (X5C5, X5C2, X5C4) or its absence (X5C0) was confirmed (Figure 1B).

Aggregate Formation by Chimeric Integrin-expressing Cells

An initial step in the formation of spheroids is cell aggregation followed by cell rearrangement and aggregate compaction (Foty *et al.*, 1994, 1996; Robinson *et al.*, 2003). This process reflects the intrinsic ability of cells to form intercellular connections with one another resulting in the formation of cellular aggregates. These aggregates, as their intercellular connections become strengthened, can compact and rearrange into spheres. To determine if the α5-integrin cytoplasmic domain is an essential requirement for α5β1-integrin–mediated aggregate formation and compaction, chi-

meric integrin-expressing cells were incubated in hanging drop assay at 2.5×10^6 cells/ml, a plating density comparable to that described for tissue engineering purposes (Mauck *et al.*, 2002; Awad *et al.*, 2003; Dvir-Ginzberg *et al.*, 2003). Cells were cultured in the absence of FN, in FN-containing serum (intermediate FN concentration; 15–30 μg/ml), or in the presence of exogenous FN (high FN concentration; 100 μg/ml). The area of the aggregate formed by each chimeric cell line was assessed using pixel quantification and was expressed relative to the empty vector control P3 cells. Aggregation and compaction was then determined and correlated with spheroid formation and aggregate cohesivity. In the absence of FN, all cells formed flat sheets (unpublished data). In the presence of intermediate FN concentrations, the wild-type, X5C0, and X5C4 cell lines formed compact aggregates that rearranged into spheroids of similar cohesivities (Figure 2A). The compaction of the X5C0 and X5C4 cells, although different from each other ($p = 0.02$), was similar to that of the wild-type ($p = 0.142$ and $p = 0.213$, respectively, Newman-Keul's test; Figure 2B). In contrast, the P3 and X5C2 cell aggregates remained loosely associated. The X5C2 cell aggregates, although more compact than the control cells, were significantly larger than those formed by the X5C5 cell line and failed to form spheroids ($p = 0.0002$; Newman-Keul's test). When cultured in a high FN concentration, all cells, with the exception of the P3 line, demonstrated a similar degree of compaction over time (unpublished data). These results demonstrate that FN is required for $\alpha5\beta1$-dependent aggregate compaction and spheroid formation. Further, these data show that the X5C2 cells are less efficient than the wild-type cells in both these processes, suggesting that they can be regulated by the $\alpha5$-integrin subunit.

The Efficiency of Spheroid Formation Does Not Correlate with FN Matrix Assembly in 2D Culture

At intermediate FN concentrations (15–30 μg/ml), we saw a significant difference in X5C2 cell aggregation and spheroid formation when compared with the X5C5 cells. As our previous work has demonstrated that FN promotes aggregate formation by $\alpha5\beta1$-expressing cells at relatively low concentrations (3 μg/ml; Robinson *et al.*, 2003), it is unlikely that FN availability alone should be a limiting step for this process.

A second requirement for $\alpha5\beta1$-integrin–mediated cohesion is that FN exists as a dimer (Robinson *et al.*, 2003). As dimeric FN is also a prerequisite for FN matrix assembly (Schwarzbauer, 1991), we hypothesized that FN matrix assembly may correlate with aggregate formation. To test this hypothesis, FN matrix assembly by the chimeric integrin-expressing cells was assessed using two methods. First, a DOC differential solubilization assay was used to quantify the assembly of fibronectin dimers into high-molecular-weight FN multimers, indicative of matrix assembly (Sechler *et al.*, 1996). The insoluble FN multimers were separated from unpolymerized FN and quantified using Western blot analysis. Second, we used fluorescence microscopy to visualize FN fibrils (Schwarzbauer, 1991). As demonstrated in Figure 3, the ability of the X5C0 cell line to assemble FN multimers in 2D culture was comparable to that of the wild-type ($p > 0.05$, Student's unpaired *t* test). Surprisingly, both the X5C4 and X5C2 cell lines were deficient in FN multimer assembly ($p < 0.05$, Student's *t* test; Figure 3, B and C). Matrix assembly was not detected in the P3 cells (Figure 3A). Organized FN fibrils were detected by immunofluorescence in the chimeric cells, confirming the presence of FN matrix assembly, but were not detected in the control P3 cells (unpublished data). These data demonstrate that the ability of cells to assemble FN into fibrils in 2D culture does not correlate with the efficiency of aggregate formation or compaction.

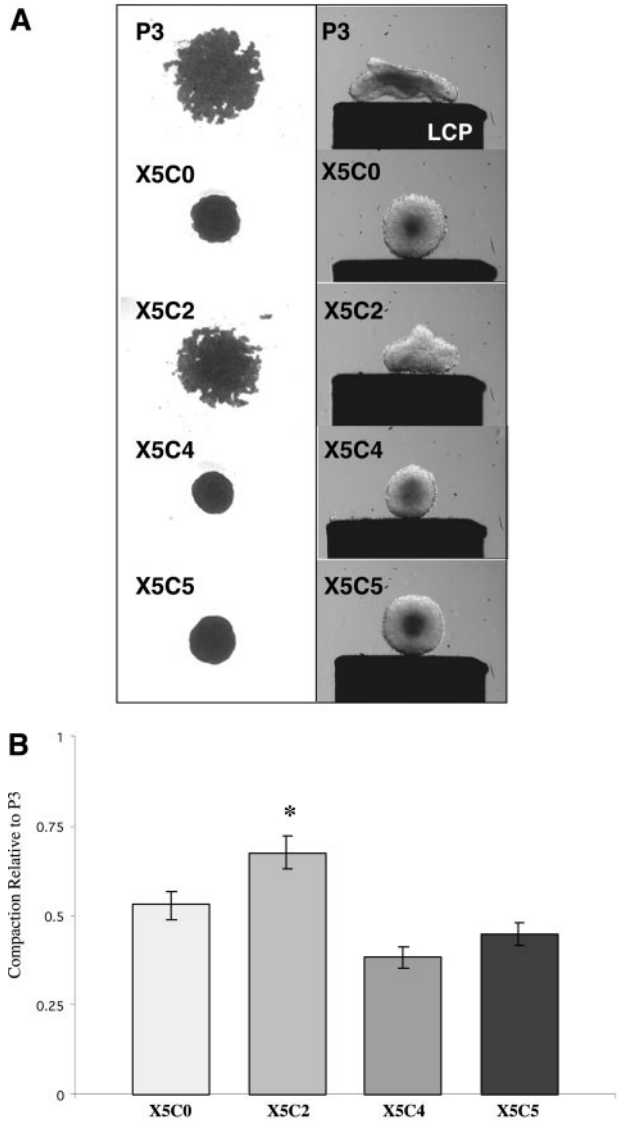

Figure 2. Aggregate formation by chimeric integrin-expressing cells. The chimeric integrin-expressing cells (2.5×10^6 cells/ml) were cultured in hanging drop assay for 2–3 d in FN-containing medium as described in MATERIALS AND METHODS. Aggregates were viewed using inverted bright field optics and images were captured using a spot camera connected to a MacIntosh G4 computer. Alternately, cell aggregates generated in hanging drop culture were transferred to shaker flasks and incubated in an orbital shaker for 2–3 d to allow for cell rearrangement and spheroid formation. Aggregate profiles are depicted on the lower compression plate (LCP) of the tensiometer as described in Robinson *et al.* (2003) (A). Pixel quantification of the aggregate images was performed using IPLabs imaging software and was expressed relative to the control P3 cells (B). Results are presented as the mean pixel value ± SEM of at least three separate experiments. *Statistical significance ($p \leq 0.05$ vs. P3 cells) as determined by a one-way ANOVA followed by a Neuman-Keuls test.

FN Matrix Assembly in 3D Culture Correlates with the Efficiency of Spheroid Formation

Although FN matrix assembly in 2D did not correlate with the efficiency of spheroid formation, cells grown in 2D cul-

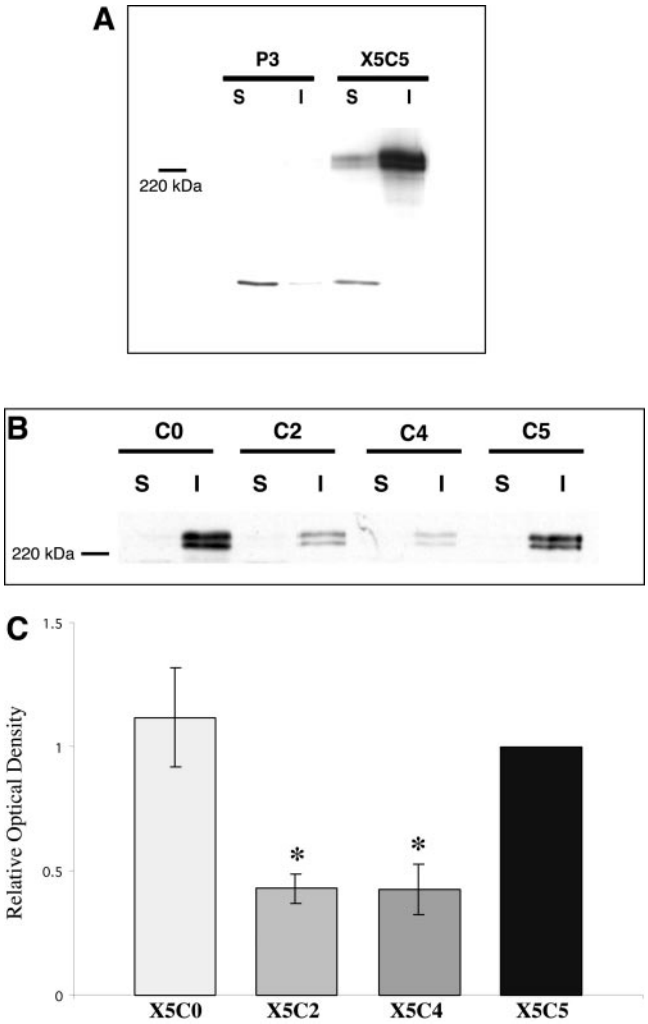

Figure 3. FN matrix assembly in 2D culture does not correlate with aggregate compaction. The assembly of high-molecular-weight FN multimers by the P3, X5C5, X5C4, X5C2, and X5C0 cell lines was assessed using DOC differential solubilization assay. DOC-soluble and -insoluble fractions were separated and analyzed by immunoblotting. Matrix assembly of X5C5 cells was compared with P3 cells (A) and to the chimeric cells lines (B). Representative immunoblots are shown. Results for B were quantified by scanning densitometry using NIH Image software and expressed relative to the X5C5 cell line (C). A P3 signal was not detected and therefore, not included. The mean values ± SEM were calculated from at least three separate experiments. *Statistical significance ($p \leq 0.05$ vs. X5C5 cells) as determined by a Student's unpaired *t* test.

ture often differ in shape, signaling, and behavior from those grown in a 3D system (Cukierman *et al.,* 2002). For this reason, the ability of the chimeric integrin-expressing cells to assemble high-molecular-weight FN multimers in hanging drop culture was also assessed (Figure 4A and B). Interestingly, only the X5C2 cell line exhibited consistently diminished levels of multimer assembly when compared with the wild-type ($p < 0.05$, Student's unpaired *t* test; Figure 4C). The level of FN multimers assembled by both the X5C0 and X5C4 was similar to that of the X5C5 cells ($p > 0.05$, Student's unpaired *t* test). The P3 cells did not assemble FN multimers in hanging drop culture (Figure 4A). These data indicate that the efficiency of FN matrix assembly by the chimeras correlates with the efficiency of spheroid formation and compaction. Further, they demonstrate that the growth of cells in the absence of external mechanical support influences the ability of the chimeric integrins to support FN matrix assembly.

The X5C5, X5C2, and P3 cell lines were also cultured as hanging drops in the presence of rhodamine-labeled FN in order to detect the presence of organized FN fibril assembly within these aggregates. As demonstrated in Figure 5A, P3 cell aggregates bind minimal FN. In contrast, an organized branching network of FN fibrils was observed in the X5C5 cell aggregates, with fibrils extending between cells in an interconnected 3D meshwork (Figure 5B). FN was also visible in the X5C2 cell aggregates; however, the fibrils were considerably shorter, with a more punctate pattern. The FN remained localized at the cell surface and rarely extended between cells (Figure 5C). These data show conclusively that cells cultured in hanging drops can assemble a FN matrix in the absence of external mechanical support. Further, it demonstrates that the ability of cells to assemble a FN matrix correlates with the efficiency of aggregate compaction.

Inhibition of FN Matrix Assembly Blocks Aggregate Compaction and Spheroid Formation

The X5C2 cell line is unique among the chimeric integrin-expressing cells in that it is less efficient both in its assembly of high-molecular-weight FN multimers in hanging drop culture and in spheroid formation. Therefore, we hypothesized that FN matrix assembly may play a key role in spheroid formation and cohesivity. To test this hypothesis, we used CHO-α5 cells. These cells have the ability to assemble a FN matrix, but only when exogenous FN is added. Moreover, they do not express cadherin, and therefore are only held together through integrin-ECM interactions (Robinson *et al.,* 2003). CHO-α5 cells were incubated with FN in hanging drop culture in the presence or absence of a 70-kDa amino-terminal FN fragment that interferes with FN matrix assembly (McKeown-Longo and Mosher, 1985). In the absence of the 70-kDa fragment, CHO-α5 cells formed compact aggregates, an initial step in spheroid formation (Figure 6A). In contrast, cells incubated with 70-kDa formed loosely associated sheets that were easily disrupted (Figure 6B). To confirm that the presence of 70 kDa was interfering with FN matrix formation, a DOC differential solubilization assay and Western blot analysis was used to detect the relative presence of FN multimers in the hanging drop cultures (Figure 6C). Incubation with 70 kDa resulted in a significant decrease in the FN matrix assembly by the CHO-α5 cells ($p < 0.05$, Student's *t* test; Figure 6D). Taken together, these results demonstrate that FN matrix assembly within 3D cell aggregates plays an essential role in $\alpha5\beta1$-integrin–mediated aggregate formation, compaction, and subsequent spheroid formation.

To determine whether FN matrix assembly could promote aggregate formation by cells that both endogenously secrete FN and express $\alpha5\beta1$, we used HT-1080 human fibrosarcoma cells. Previous work has indicated that FN matrix assembly by these cells is enhanced by pretreatment with dexamethasone(Brenner *et al.,* 2000). However, HT-1080 cells cultured in 3D form high-molecular-weight FN multimers in the absence of dexamethasone (Figure 7A). Therefore, the remaining experiments were performed without the addition of dexamethasone.

HT-1080 cells incubated in hanging drop culture aggregate (Figure 7B) and become more compact when exogenous FN is added (Figure 7C). Addition of the 70-kDa fragment interfered with both aggregation and compaction, resulting in loosely associated cell clusters (Figure 7, D and E). These

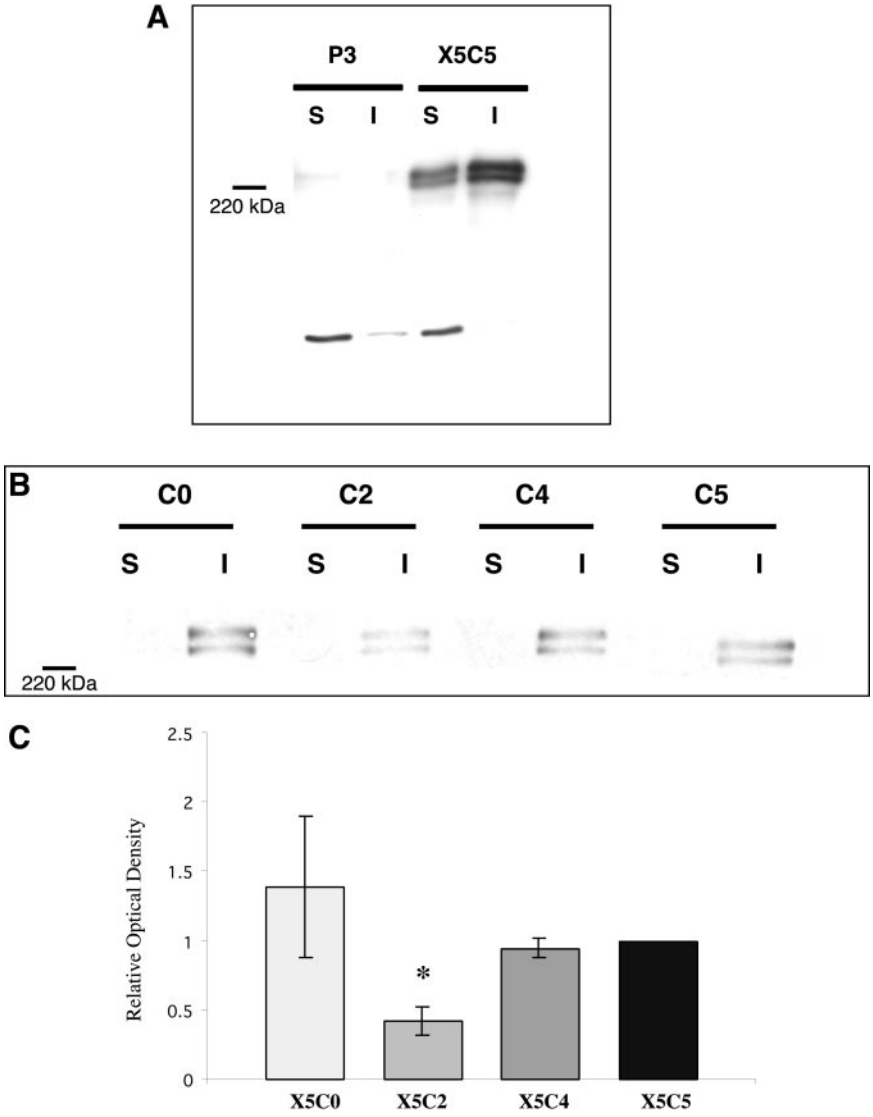

Figure 4. FN matrix assembly in 3D culture correlates with aggregate compaction. P3, X5C5, X5C4, X5C2, and X5C0 cell lines were cultured as hanging drops for 16 h in the presence of 100 μg/ml exogenous rat plasma FN under tissue culture conditions. Aggregates were then harvested and the assembly of high-molecular-weight FN multimers was assessed as described in Figure 3. Matrix assembly of X5C5 cells in 3D culture was compared with P3 cells (A) and with the chimeric cells lines (B). Representative immunoblots are shown. Results for B were quantified by scanning densitometry using NIH Image software and expressed relative to the X5C5 cell line (C). A P3 signal was not detected and therefore, not included. The mean values ± SEM were calculated from at least three separate experiments. *Statistical significance ($p \leq 0.05$ vs. X5C5 cells) as determined by a Student's unpaired *t* test.

data support the physiological role of FN matrix assembly in promoting the intercellular associations required for spheroid formation and cohesivity.

DISCUSSION

In this article, we have used chimeric integrin-expressing cells cultured in hanging drops to investigate the functional role of the α5-integrin subunit in $\alpha5\beta1$-integrin–mediated cell aggregation, spheroid formation, and cohesivity. These data demonstrate that 1) $\alpha5\beta1$-expressing cells can assemble a FN matrix when cultured as multilayered aggregates in the absence of rigid mechanical support, 2) FN matrix assembly by the chimeric cells correlates with efficient cell aggregation, compaction, and spheroid formation, 3) inhibition of FN matrix assembly blocks the intercellular associations required for spheroid formation and cohesion, and 4) $\alpha5\beta1$-mediated FN fibrillogenesis is regulated by the 3D environment. An understanding of the role of $\alpha5\beta1$-mediated FN matrix assembly in tissue cohesion and the factors that influence this process is fundamental to the development of suitable in vitro models that approximate cell behavior and function in a 3D context.

FN matrix assembly is traditionally studied in a 2D system in which cells are adherent and spread. The interaction between β-integrin and an intact cytoskeleton as well as the assembly of actin stress fibers and cell-generated tension are all thought to be important factors supporting FN matrix assembly (Hynes, 1990; Halliday and Tomasek, 1995; Wu *et al.*, 1995). FN matrix assembly has also been demonstrated in a 3D system. For example, Halliday and Tomasek (1995) have demonstrated FN fibril and stress fiber formation by fibroblasts cultured in attached collagen gels. Similarly, using floating collage gels, Hocking *et al.* (2000) demonstrated that fibroblasts were able to spread, generate tension, and polymerize FN within this 3D ECM scaffold . We have demonstrated that the X5C5 cells generate both DOC insoluble high-molecular-weight FN multimers in 3D, hanging drop culture and a branching network of FN fibrils that link adjacent cells. To our knowledge, this is the first demonstration of de novo FN fibril assembly in an in vitro culture system under conditions of minimal mechanical stress. As such, it provides a novel model with which to examine the mechanisms of FN fibril formation in a more physiologically relevant context.

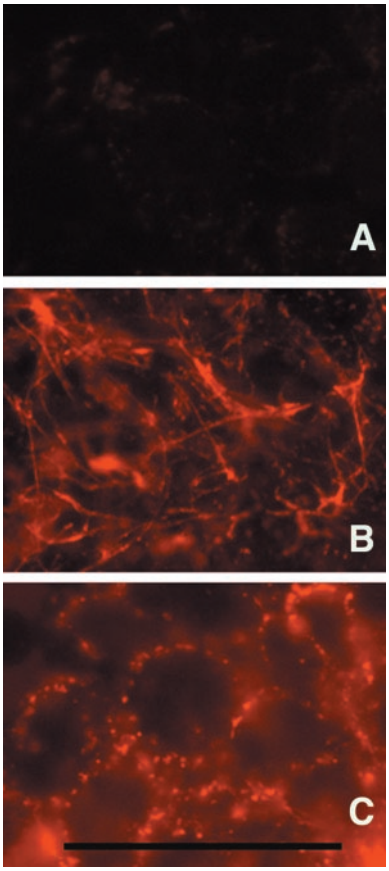

Figure 5. X5C2 cells do not form fibrils in 3D culture. P3 (A), X5C5 (B), and X5C2 (C) cells were trypsinized from near-confluent plates and resuspended at 2.5 × 10^6 cells/ml in FN-depleted medium (Corbett *et al.,* 1997). Cells were incubated in the presence of 30 μg/ml rhodamine-labeled FN in 15-μl hanging drops for 24 h under tissue culture conditions. Hanging drops were then transferred to glass coverslips and visualized using inverted fluorescent optics. Bar, 20 μm.

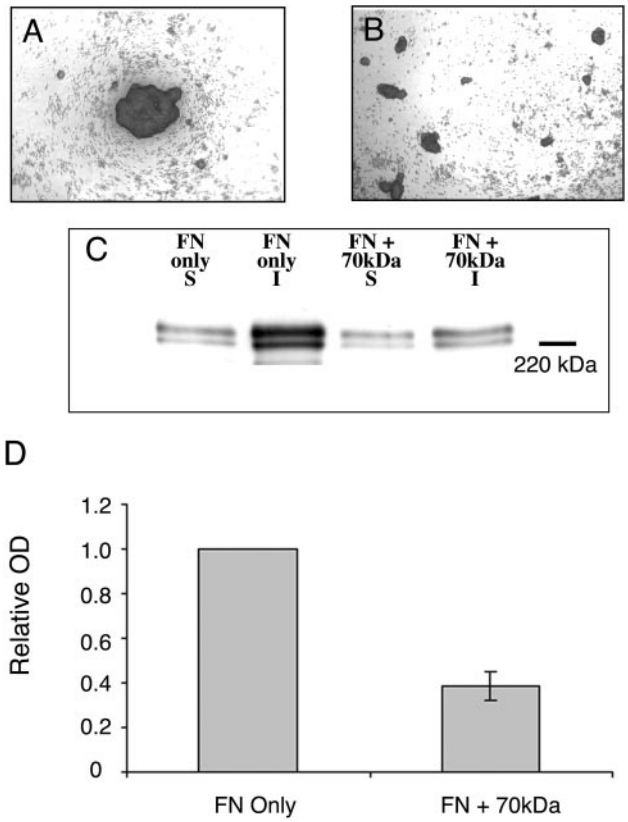

Figure 6. Inhibition of FN matrix assembly by the 70-kDa FN fragment inhibits CHO-α5 aggregate formation. CHO-α5 cells (2.5 × 10^6 cells/ml) were cultured in hanging drop assay in medium supplemented with 50 μg/ml FN, in the presence (B) or absence (A) of 25 μg/ml the 70-kDa amino-terminal FN fragment. Aggregates were viewed using inverted bright field optics. Alternately, hanging drops were harvested and the assembly of high-molecular-weight FN multimers assessed as described in Figure 3. (C) A representative immunoblot. In D, results were quantified by scanning densitometry using NIH Image software and expressed relative to the X5C5 cell line. The mean values ± SEM were calculated from at least three separate experiments. *Statistical significance ($p \leq 0.05$ vs. X5C5 cells) as determined by a Student's unpaired *t* test.

Using fibroblasts cultured in relaxed and stressed collagen gels, it has been demonstrated that cell-generated tension is required for FN matrix assembly (Halliday and Tomasek, 1995). These data support the well-described association of actin stress fiber formation with matrix assembly (Hynes, 1990; Sechler and Schwarzbauer, 1997). Recent work by Ohashi *et al.* (2002) used fluorescence microscopy to visualize actin patterns and FN fibril assembly over time by sparsely plated cells. They demonstrated that FN initially adheres over an activated β1-integrin and actin bundle. These spots then grow into patches and fibrils. The authors noted that with fibril elongation, the FN became adherent and anchored to the solid surface of the tissue culture dish. In our culture system, no surface exists for FN adhesion other than the cells themselves, and all fibrils visualized were generated between cells, without the involvement of a solid substrate. This suggests that cell-FN-cell interactions can generate sufficient tension to support FN fibril assembly in the absence of both FN-substrate and cell-substrate adhesion. In addition, this lack of rigid substrate to assist in tension generation may partially explain why the fibrillar network assembled by the X5C5 cells in cell aggregates was less extensive than the dense matrix generated in 2D at 24 h.

Evidence exists in the literature to support the varied influence of 3D vs. 2D culture systems on a variety of cellular processes. For example, breast cancer cells grown in reconstituted basement membrane 3D matrices have been demonstrated to differ in morphology, growth, and gene expression from those grown as 2D monolayers (Weaver *et al.,* 1997). In addition, using both "tissue-derived" and "cell-derived" 3D matrices, it has been demonstrated that the cell adhesion, migration, and proliferation of human fibroblasts cultured on 3D matrices differed when compared with those cultured on 2D ligand-coated surfaces (Cukierman *et al.,* 2001). In our experiments, the transition from 2D culture to multilayered aggregates enhanced FN matrix assembly by the X5C4 cells. This supports the idea that the microenvironment can influence α5β1-mediated FN fibril formation. Our experiments with HT-1080 cells confirm these results. These cells are unable to naturally assemble FN multimers in 2D culture, but readily do so when cultured as aggregates. Increased matrix assembly in this context can promote cell aggregation, spheroid formation, and cohesion by creating a scaffold that links the cells and provides an adhesive 3D

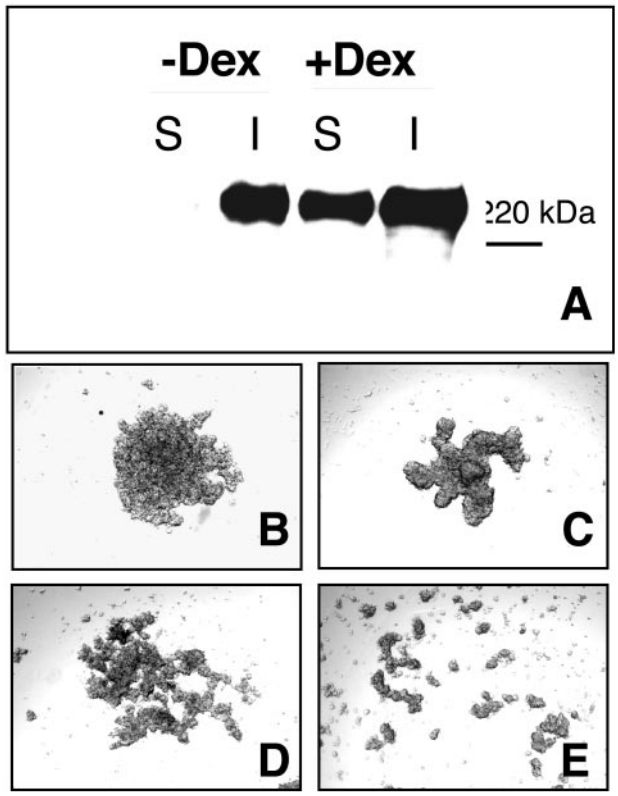

Figure 7. The 70-kDa FN fragment inhibits HT1080 aggregate formation. HT1080 cells (2.5×10^6 cells/ml) were cultured in hanging drop assay in the presence or absence of 10^{-7} M dexamethasone (A). Hanging drops were harvested and the assembly of high-molecular-weight FN multimers assessed as described in Figure 3. In separate experiments, HT1080 cells were cultured in FN-depleted medium (B and D) or medium supplemented with 50 μg/ml FN (C and E). The 70-kDa amino-terminal FN fragment (25 μg/ml) was added to inhibit matrix assembly (D and E). Aggregates were viewed using inverted bright field optics.

matrix to support tissue compaction and remodeling. This emphasizes the importance of considering dimensionality in predicting integrin function and the potential contribution of integrin-ECM interactions to tissue cohesion.

The data presented in this article demonstrate a role for FN matrix assembly in 3D spheroid formation. In this model, cells adhere to available FN dimers that can inherently link two adjacent cells. The net effect of integrin-FN interactions in 3D is force generation and cellular rearrangement into a close-packed, spherical conformation. A logical corollary to this hypothesis is that increased matrix assembly could lead to increased compaction and cohesivity. Similarly, loss of FN matrix, either through decreased $\alpha5\beta1$ or FN expression or through matrix degradation, could result in increased cell dispersal. This has important implications for a variety of cellular processes. For example, in the early stages of wound healing, abundant FN is deposited in the granulation tissue during a time when cells upregulate $\alpha5\beta1$ expression (Grinnell *et al.*, 1981; Clark, 1990). The early organization of a FN matrix can initiate the process of contraction and remodeling, before the deposition of collagen. Further, factors that contribute to increased FN deposition could promote tension generation, accelerating compaction and altering the behavior of cells responding to force cues.

In vertebrate limb development, FN levels rise during the condensation of chondrogenic precursors at the future sites of bone formation (Tomasek *et al.*, 1982). FN deposition is accompanied by the aggregation of the precartilage mesenchymal cells, both in vivo and in vitro. Treatment of freshly isolated embryonic wing cultures with an anti-FN antibody that disrupts FN matrix assembly results in condensations in which the cells are more loosely organized and decreases chondrogenesis by ~50% (Downie and Newman, 1995). These data support our in vitro observations that correlate FN matrix assembly with cell aggregation. Moreover, it suggests that FN expression can provide morphogenetic cues during development by influencing the strength of intercellular associations.

In conclusion, we demonstrate that FN matrix assembly plays a key role in cell aggregation, spheroid formation, and cohesion. Further, we show that the ability of cells to support FN fibrillogenesis is regulated by the microenvironment. Understanding the mechanism of $\alpha5\beta1$-mediated FN matrix assembly its role in regulating tissue cohesion can help to provide further insight into the factors that regulate this essential cellular process in vivo.

REFERENCES

Adamska, M., MacDonald, B.T., and Meisler, M.H. (2003). Doubleridge, a mouse mutant with defective compaction of the apical ectodermal ridge and normal dorsal-ventral patterning of the limb. Dev. Biol. *255,* 350–362.

Akamatsu, H., Ichihara-Tanaka, K., Ozono, K., Kamiike, W., Matsuda, H., and Sekiguchi, K. (1996). Suppression of transformed phenotypes of human fibrosarcoma cells by overexpression of recombinant fibronectin. Cancer Res. *56,* 4541–4546.

Akiyama, S.K., Aota, S., and Yamada, K.M. (1995). Function and receptor specificity of a minimal 20 kilodalton cell adhesive fragment of fibronectin. Cell Adhes. Commun. *3,* 13–25.

Armstrong, P.B., and Armstrong, M.T. (2000). Intercellular invasion and the organizational stability of tissues: a role for fibronectin. Biochim. Biophys. Acta *1470,* O9–O20.

Awad, H.A., Boivin, G.P., Dressler, M.R., Smith, F.N., Young, R.G., and Butler, D.L. (2003). Repair of patellar tendon injuries using a cell-collagen composite. J. Orthop. Res. *21,* 420–431.

Berry, D.P., Harding, K.G., Stanton, M.R., Jasani, B., and Ehrlich, H.P. (1998). Human wound contraction: collagen organization, fibroblasts, and myofibroblasts. Plast. Reconstr. Surg. *102,* 124–131; discussion 132–124.

Brenner, K.A., Corbett, S.A., and Schwarzbauer, J.E. (2000). Regulation of fibronectin matrix assembly by activated Ras in transformed cells. Oncogene *19,* 3156–3163.

Clark, R.A. (1990). Fibronectin matrix deposition and fibronectin receptor expression in healing and normal skin. J. Invest. Dermatol. *94,* 128S–134S.

Corbett, S.A., Lee, L., Wilson, C.L., and Schwarzbauer, J.E. (1997). Covalent cross-linking of fibronectin to fibrin is required for maximal cell adhesion to a fibronectin-fibrin matrix. J. Biol. Chem. *272,* 24999–25005.

Corbett, S.A., and Schwarzbauer, J.E. (1999). Requirements for alpha(5)beta(1) integrin-mediated retraction of fibronectin-fibrin matrices. J. Biol. Chem. *274,* 20943–20948.

Cukierman, E., Pankov, R., Stevens, D.R., and Yamada, K.M. (2001). Taking cell-matrix adhesions to the third dimension. Science *294,* 1708–1712.

Cukierman, E., Pankov, R., and Yamada, K.M. (2002). Cell interactions with three-dimensional matrices. Curr. Opin. Cell Biol. *14,* 633–639.

Downie, S.A., and Newman, S.A. (1995). Different roles for fibronectin in the generation of fore and hind limb precartilage condensations. Dev. Biol. *172,* 519–530.

Dvir-Ginzberg, M., Gamlieli-Bonshtein, I., Agbaria, R., and Cohen, S. (2003). Liver tissue engineering within alginate scaffolds: effects of cell-seeding density on hepatocyte viability, morphology, and function. Tissue Eng. *9,* 757–766.

Fleming, T.P., Sheth, B., and Fesenko, I. (2001). Cell adhesion in the preimplantation mammalian embryo and its role in trophectoderm differentiation and blastocyst morphogenesis. Front. Biosci. *6,* D1000–D1007.

Folkman, J., and Moscona, A. (1978). Role of cell shape in growth control. Nature *273,* 345–349.

Foty, R.A., Forgacs, G., Pfleger, C.M., and Steinberg, M.S. (1994). Liquid properties of embryonic tissues: measurement of interfacial tensions. Phys. Rev. Lett. *72,* 2298–2301.

Foty, R.A., Pfleger, C.M., Forgacs, G., and Steinberg, M.S. (1996). Surface tensions of embryonic tissues predict their mutual envelopment behavior. Development *122,* 1611–1620.

Grinnell, F., Billingham, R.E., and Burgess, L. (1981). Distribution of fibronectin during wound healing in vivo. J. Invest. Dermatol. *76,* 181–189.

Halliday, N.L., and Tomasek, J.J. (1995). Mechanical properties of the extracellular matrix influence fibronectin fibril assembly in vitro. Exp. Cell Res. *217,* 109–117.

Hocking, D.C., Sottile, J., and Langenbach, K.J. (2000). Stimulation of integrin-mediated cell contractility by fibronectin polymerization. J. Biol. Chem. *275,* 10673–10682.

Hocking, D.C., Sottile, J., and McKeown-Longo, P.J. (1994). Fibronectin's III-1 module contains a conformation-dependent binding site for the amino-terminal region of fibronectin. J. Biol. Chem. *269,* 19183–19187.

Hynes, R.O. (1990). Fibronectins. Springer-Verlag: New York.

Khan, I.A., Biddle, W.P., Najeed, S.A., Abdul-Aziz, S., Mehta, N.J., Salaria, V., Murcek, A.L., and Harris, D.M. (2003). Isolated noncompaction cardiomyopathy presenting with paroxysmal supraventricular tachycardia—case report and literature review. Angiology *54,* 243–250.

Lash, J.W., Seitz, A.W., Cheney, C.M., and Ostrovsky, D. (1984). On the role of fibronectin during the compaction stage of somitogenesis in the chick embryo. J. Exp. Zool. *232,* 197–206.

Mauck, R.L., Seyhan, S.L., Ateshian, G.A., and Hung, C.T. (2002). Influence of seeding density and dynamic deformational loading on the developing structure/function relationships of chondrocyte-seeded agarose hydrogels. Ann. Biomed. Eng. *30,* 1046–1056.

McKeown-Longo, P.J., and Mosher, D.F. (1985). Interaction of the 70,000-mol-wt amino-terminal fragment of fibronectin with the matrix-assembly receptor of fibroblasts. J. Cell Biol. *100,* 364–374.

Morla, A., and Ruoslahti, E. (1992). A fibronectin self-assembly site involved in fibronectin matrix assembly: reconstruction in a synthetic peptide. J. Cell Biol. *118,* 421–429.

Ohashi, T., Kiehart, D.P., and Erickson, H.P. (2002). Dual labeling of the fibronectin matrix and actin cytoskeleton with green fluorescent protein variants. J. Cell Sci. *115,* 1221–1229.

Richa, J., Damsky, C.H., Buck, C.A., Knowles, B.B., and Solter, D. (1985). Cell surface glycoproteins mediate compaction, trophoblast attachment, and endoderm formation during early mouse development. Dev. Biol. *108,* 513–521.

Robinson, E.E., Zazzali, K.M., Corbett, S.A., and Foty, R.A. (2003). alpha5beta1 integrin mediates strong tissue cohesion. J. Cell Sci. *116,* 377–386.

Schreiner, C.L., Bauer, J.S., Danilov, Y.N., Hussein, S., Sczekan, M.M., and Juliano, R.L. (1989). Isolation and characterization of Chinese hamster ovary cell variants deficient in the expression of fibronectin receptor. J. Cell Biol. *109,* 3157–3167.

Schwarzbauer, J.E. (1991). Identification of the fibronectin sequences required for assembly of a fibrillar matrix. J. Cell Biol. *113,* 1463–1473.

Sechler, J.L., and Schwarzbauer, J.E. (1997). Coordinated regulation of fibronectin fibril assembly and actin stress fiber formation. Cell Adhes. Commun. *4,* 413–424.

Sechler, J.L., Takada, Y., and Schwarzbauer, J.E. (1996). Altered rate of fibronectin matrix assembly by deletion of the first type III repeats. J. Cell Biol. *134,* 573–583.

Tomasek, J.J., Mazurkiewicz, J.E., and Newman, S.A. (1982). Nonuniform distribution of fibronectin during avian limb development. Dev. Biol. *90,* 118–126.

Weaver, V.M., Petersen, O.W., Wang, F., Larabell, C.A., Briand, P., Damsky, C., and Bissell, M.J. (1997). Reversion of the malignant phenotype of human breast cells in three-dimensional culture and in vivo by integrin blocking antibodies. J. Cell Biol. *137,* 231–245.

Wierzbicka-Patynowski, I., and Schwarzbauer, J.E. (2003). The ins and outs of fibronectin matrix assembly. J. Cell Sci. *116,* 3269–3276.

Wu, C., Keivens, V.M., O'Toole, T.E., McDonald, J.A., and Ginsberg, M.H. (1995). Integrin activation and cytoskeletal interaction are essential for the assembly of a fibronectin matrix. Cell *83,* 715–724.

Yang, J.T., and Hynes, R.O. (1996). Fibronectin receptor functions in embryonic cells deficient in alpha 5 beta 1 integrin can be replaced by alpha V integrins. Mol. Biol. Cell *7,* 1737–1748.

Yang, J.T., Rayburn, H., and Hynes, R.O. (1993). Embryonic mesodermal defects in alpha 5 integrin-deficient mice. Development *119,* 1093–1105.